Original Research Article

Functionalized nanocomposites of gold and their optical studies

Vilvamani Narayanasamy*

Assistant Professor of Chemistry Department of Chemistry Sacred Heart College (Autonomous) Tirupattur district, Tamil Nadu, India
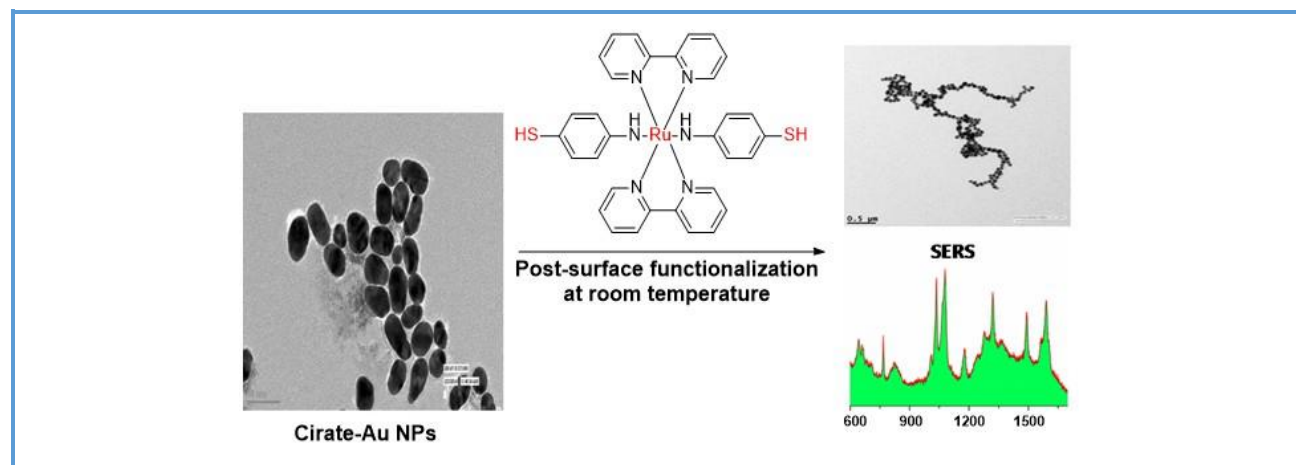
ABSTRACT

Post-functionalization strategy on gold nanoparticles (Au NPs) surface provides access to novel nanocomposite materials with specific physico-chemical properties for a variety of interdisciplinary applications. In this work, functionalized gold nanocomposites (Au NCs) with unique morphological features were achieved by utilizing Ruthenium(II)-polypyridyl complexes with various functional groups. They were synthesized by using ethanol/water medium at room temperature by place-exchange methodology. As the progress of binding Ru(II)-polypyridyl complex molecules, changed from ionic to covalent fashion, then Ru(II)-polypyridyl complex molecules-induced self-assembly was observed. This was evident in UV-Vis spectroscopic and TEM studies. Additionally, Ru(II)-polypyridyl complexes binding showed altered Au NPs surface with SERS enhancement at micromolar concentration level and Raman scattering signals of Au surface-bound Ru(II)-polypyridyl complexes were studied through a hot spot mechanism.

Graphical Abstract

Cirate-Au NPs

Post-surface functionalization at room temperature

SERS

Corresponding author, email: nvilvamani@gmail.com (V. Narayanasamy).

Introduction

Surface functionalization of metal nanoparticles (NPs) with coordination compounds has received attention in recent years. Because coordination compounds with terminal binding sites on metal NPs give novel properties like optical, electrochemical, catalytic properties, cellular imaging agents, and sensing platforms [1–3]. These functionalized metal NPs might be useful for the design of functional supramolecular assemblies [4]. Particularly, gold NPs (Au NPs) and silver NPs (Ag NPs) exhibit shape and size-dependent extraordinary optical properties comparatively with corresponding bulk materials [5]. Recently, Au NPs functionalized by a variety of coordination compounds using the high affinity of atoms such as sulfur, nitrogen and phosphorus in the capping molecules [6–8]. In addition, pH and ionic strength parameters were utilized to induce self-assemblies of gold nanoparticles. Thus, the development of nanoparticle-molecule interfaces has become a booming field of research due to its wide applications. The enhancement of SERS signals in functionalized colloidal systems is based on the molecular orientations and the structure of the nanosurface. The electromagnetic field, which is generated on the nanosurface so-called "hot spots", plays a vital role in determining the molecular structures. While binding the molecules randomLy and oriented on the nanosurface, the electromagnetic-plasmon field intensifies all the vibrational modes of the molecules [9]. In the present work, the role of binding functional Ru(II)-polypyridyl complexes and the mode of binding on Au NPs surface were studied by taking various Ru(II)-polypyridyl complexes, and the resulting functional Au NCs optical and morphological properties were studied in detail using UV-Vis, Raman spectroscopic techniques and TEM. In

[Ru(1, 10-phen)$_2$(dafo)](PF$_6$)$_2$ complex (Complex 1), 4, 5-diazafluoren-9-one (dafo) ligand binds on the surface of Au NPs through O-atom present in –C=O group, in case of [Ru(2, 2'-bpy)$_2$(IPBA)](PF$_6$)$_2$ (Complex 2), 4-(1H-imidazo [4, 5-f] [1, 10] phenanthrolin-2-yl)benzoic acid (IPBA) ligand incorporated and utilized to bound on Au NP through ionic interaction. In [Ru(1, 10-phen)$_2$(dah)](PF$_6$)$_2$ complex (Complex 3), 4,5-diazafluorenone hydrazone (dah) ligand was placed with –NH$_2$ group, which bound on Au NPs surface by replacing citrate molecules and in [Ru(2, 2'-bpy)$_2$(4-ATP)$_2$](PF$_6$)$_2$ complex (Complex 4), 4-aminothiophenol (4-ATP) ligands were bound on Au NPs surface covalently on Au NPs surface. Citrate displacement on Au NPs was proved by monitoring the stability of colloidal Au NCs solution using UV-Vis spectroscopy. Along with morphological studies, Raman spectra of Ru(II)-polypyridyl complexes of post-functionalized Au NCs were studied at lesser than microlevel concentration with a hot spot mechanism.

Experimental

Materials and method

Hydrogen tetrachloroaurate trihydrate (HAuCl$_4$.3H$_2$O, 49.99% metal basis), trisodiumcitrate dihydrate (99%), 4-aminothiophenol (4-ATP, 97%) were acquired from Alfa Aesar, Massachusetts (USA). 2,2'-bipyridine (2, 2'-bpy, 99%), RuCl$_3$.xH$_2$O (99.98%) were received from Sigma-Aldrich, 1, 10-phenanthroline (1, 10-phen, 99%) from Spectrochem, hydrazine monohydrate (N$_2$H$_4$.H$_2$O, 99%), diethyl ether (99%), acetonitrile (HPLC) were acquired from Rankem (India), 4,5-diazafluoren-9-one (dafo) [10], cis-bis (2, 2'-bpy)$_2$RuCl$_2$.2H$_2$O and cis-bis (1, 10-phen)$_2$RuCl$_2$.2H$_2$O [11], Ru(2,2'-bpy)$_2$(IPBA).2PF$_6$ and Ru(1, 10-phen)$_2$(IPBA).2PF$_6$ [12], Ru(1, 10-

phen)$_2$(dafo).2PF$_6$ [13]. For making aqueous solutions milliQ water was used unless specified elsewhere.

Preparation of citrate capped Au NPs

Citrate capped Au NPs were freshly prepared by the standard citrate reduction method. In this typical experiment, 2.5 mL of trisodium citrate (38.8 mM) was rapidly injected into a boiling solution of HAuCl$_4$ (25 mL, 1 mM), and the resulting solution was further refluxed for another 25 minutes into a wine-red suspension. The suspension was gradually cooled to room temperature naturally under stirred condition for another 30 minutes, and stored at 4 °C for further use [14].

Preparation of functionalized gold nanocomposites for optical and morphological studies

All Ru(II)-polypyridyl complex functionalized Au NCs were prepared by adding complex 1-4 with specific concentrations ([Ru(1, 10-phen)$_2$(dafo)](PF$_6$)$_2$ complex1: 5.0 µM, [Ru(2, 2'-bpy)$_2$(IPBA)](PF$_6$)$_2$ complex2: 1.0×10^{-4} M, [Ru(1,10-phen)$_2$(dah)](PF$_6$)$_2$ complex3: 5.0 µM [Ru(2, 2'-bpy)$_2$(4-ATP)$_2$](PF$_6$)$_2$ complex4:1×10^{-7} M) 5 µL/addition to citrate capped Au NPs (5 mL) at room temperature, was added dropwise with constant stirring for 2 hours in ACN:H$_2$O (1:1 v/v) solvent mixture, spectroscopically monitored and then centrifuged to make them free from unbound Ru(II)-polypyridyl complexes and was washed in ACN:H$_2$O (1:1 v/v) solvent mixture twice. The resulting functionalized Au NCs 1-4 were dispersed again in ACN:H$_2$O (1:1 v/v) solvent mixture for optical studies and then deposited over carbon-coated TEM grid to a make thin layer of functionalized Au NCs for morphological studies.

Instrumentation

Morphological features of post-surface functionalized Au NCs were studied by using high-resolution transmission electron microscopy (HRTEM, TECNAI G2 T30) working at 300 kV accelerating voltage coupled with an EDS facility. Electronic absorption spectra of samples were recorded by using Jasco V-670 spectrophotometer at room temperature. Raman scattering studies were carried out by using a Horiba Jobin Yvon LabRam HR 800 system operating at laser excitation of 488 nm and Renishaw invia Raman spectrometer operating at laser excitation of 785 nm (HPNIR diode).

Results and Discussion

Morphological studies of post-functionalized Au nanocomposites (Au NCs)

Citrate-capped Au NPs were reacted with complex 1-4 at room temperature in ACN:H$_2$O (1:1 v/v) mixture and observed the formation of Au nanocomposites (Au NCs) formation with time. The resulting Au NCs showed modified morphological features with respect to the nature of the complex molecules introduced in the citrate-capped Au NPs colloidal solution. Invariably, all the Ru(II)-polypyridyl complex molecules (Complex **1-4**) (Figure 1) replaced citrate anions bound on Au NPs surface in different modes of binding on the Au surface. This post-functionalization was confirmed by UV-Vis spectra studies and TEM viewing studies.

The post-functionalization of complex1 (5.0 µM) over citrate capped Au NPs (5 mL) was performed at room temperature and the surface-modified Au NCs morphology was changed from spherical to Au NC random aggregates (Figure 2**a** and 2**b**). UV-Vis spectra confirmed the formation of Au NCs with altered

morphology by replacing citrate molecules on Au NPs surface and surface Plasmon resonance (SPR) of citrate capped Au NPs (520 nm) was shifted slightly towards a longer wavelength and the bathochromic shift was observed. This confirmed the ability of –C=O functionality which was presented in complex1 molecule, which could stabilize the surface crystal planes of Au-complex1 like polyvinylpyrollidone (PVP) at room temperature [15]. Further, complex 2 was bound with citrate capped Au NPs surface through a non-covalent fashion and formed a random short range assembly of Au NCs, which was observed with a length of ≤200 nm (Figure 2b). UV-vis spectra confirmed the formation of closely arranged Au NCs as they showed coupled surface Plasmon resonance at 615 nm after surface modification with complex 2. Closely arranged Au NCs particles made the particle coupled surface plasmon resonance band in complex 2-Au NCs. The presence of extended conjugation in complex 2 made the Au NCs arranged as short-length Au chains confirmed by TEM image (Figure 3c).

Complex 3 was bound with lone pair of N-atom from dah ligand and extended π-conjugation through single surface binding -NH₂ site induced weak covalent interaction on citrate capped Au NP surface (Figure 2c). The extension of π-conjugation in complex 3 influenced optical response was confirmed by comparing UV-Vis spectra of Au-complex 1.

A strong bathochromic shift was noted while binding complex 3 on the Au surface. TEM imaging process also confirmed the functionality dependant morphology formation process and formed scattered Au NCs (S3 (Supporting Information)). Furthermore, the surface modification of citrate-capped Au NPs was carried out by the addition of 1×10^{-7} M Complex 4 (5 μL/addition). Step-wise addition of complex 4 changed the surface of citrate-Au NPs and formed one-dimensional chain Au NC assemblies evident by coupled surface plasmon resonance with bathochromic shift up to 670 nm due to the assembly of Au NC particles (Figure 2d).
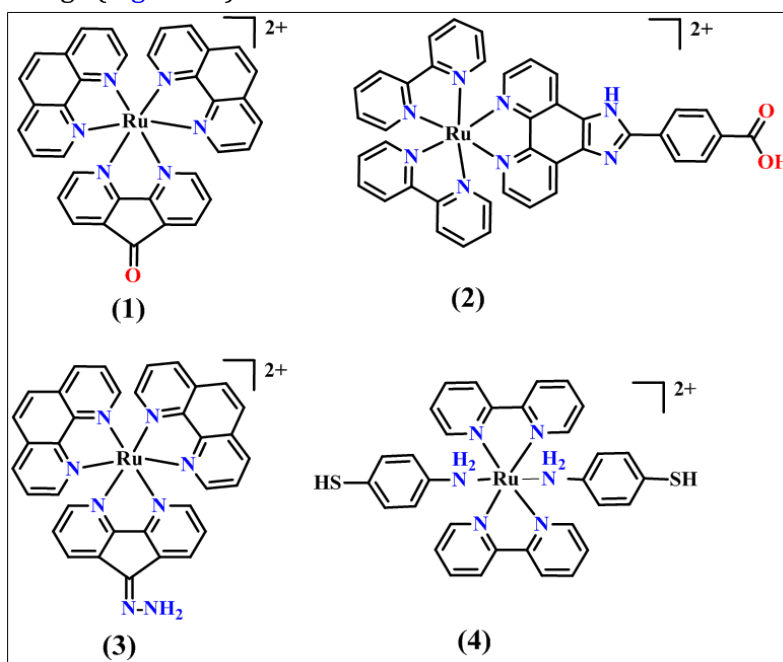

Figure 1. Molecular structure of Ru(II)-polypyridyl complexes with counter anion 2PF₆ (Complex **1-4**)
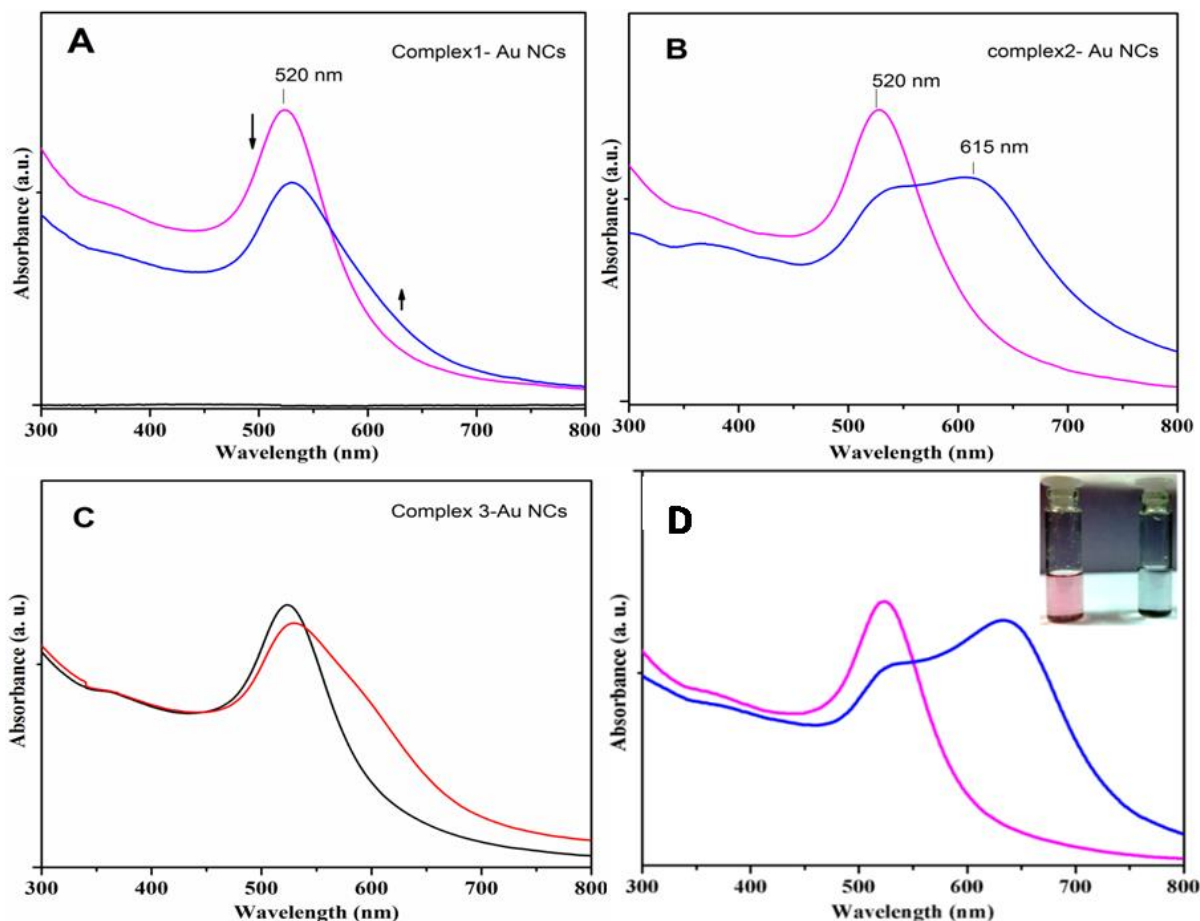
Figure 2. a) UV-vis spectra profile of citrate capped Au NPs SPR position before (pink line–λ_{max}=520 nm) and after functionalization with complex **1** with bathochromic shift (blue line), b) citrate capped Au NPs SPR position before (pink line-λ_{max}=520 nm) and after the surface functionalization with complex **2** (blue line-λ_{max}=615 nm), c) UV-vis spectra profile of citrate capped Au NPs before (black line-λ_{max}=520 nm) and after the surface functionalization with complex **3** with bathochromic shift (red line), UV-vis spectra profile of citrate capped Au NPs SPR position before (pink line) and after functionalization with complex **4** (blue line-λ_{max}=670 nm) and inset: Digital image showing visible colour change before and after surface functionalization with complex **4**

UV-vis spectra and TEM image clearly showed the replacement of citrate molecules removal and complex **4** binding on Au NC particle surface. Further, the Au NCs arranged in one dimensional way up to the micrometer scale (Figure 3**d**). The presence of complex4 and crystallinity of Au NCs were confirmed by EDS and SAED studies (S4, Supporting Information). Thus, the replacement of electrostatically bound citrate happened preferably by 4-ATP ligand of complex-4 on Au NP surface pseudo-covalently (~45 K cal/mol) [16]. This covalent binding nature of 4-ATP incorporated complex **4** showed unique responses in Raman scattering studies are discussed below.
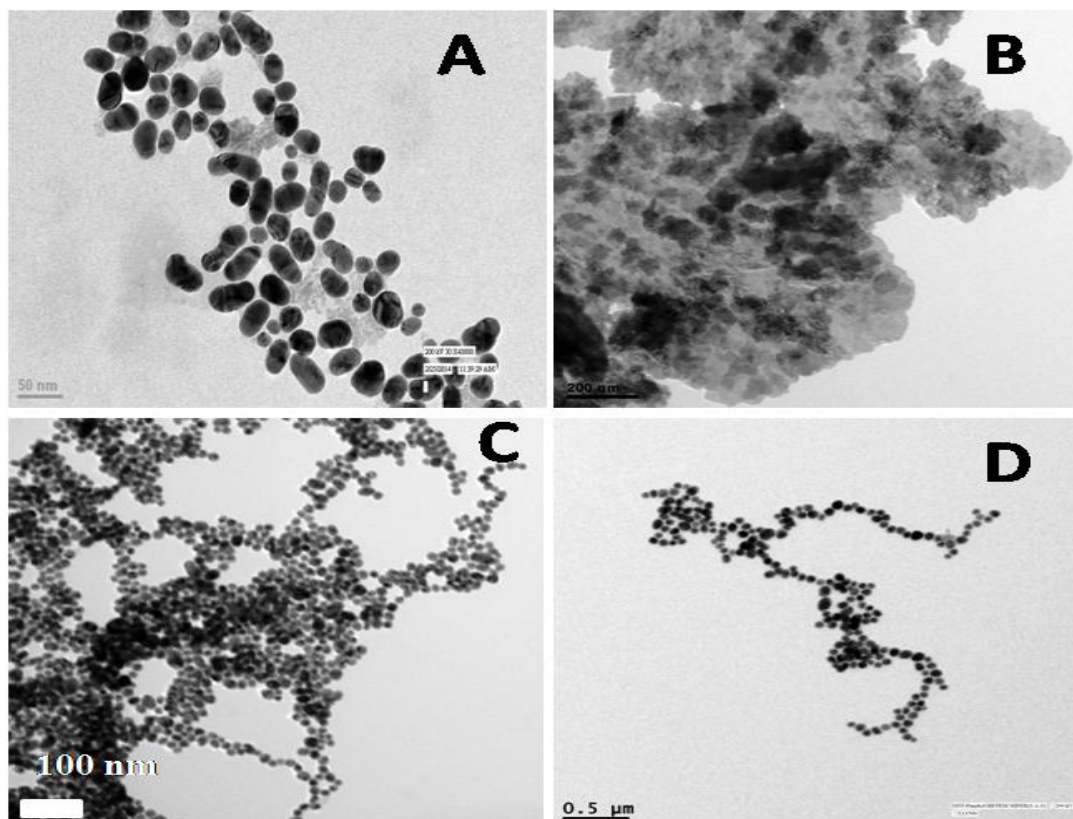
Figure 3. a) TEM view of citrate capped-Au nanoparticles before surface functionalization, b) TEM view of Au-Complex **1** aggregated with complex **1** (5.0 µM), c) TEM view of Au-complex **2** short-range Au NC chains with complex 2 (1.0×10^{-4} M), d) TEM view of Au-Complex **4** Au NC chains with complex **4** (1× 10^{-7} M)

Surface enhanced raman scattering (SERS) studies of Au NCs

The vibrational bands originated from functionalized Ru(II)-polypyridyl complexes on Au NCs are utilized to prove their surface binding capability through the possible modes of interaction with a specific functional group. Functionalized Ru(II)-polypyridyl complex **1-4** were examined to probe the molecular structural information on Au NC particle surface by recording Raman spectral bands at the excitation wavelengths of 488 and 785 nm. The carbonyl group from complex **1** might be bound on Au NPs through the oxygen atom in a donor-acceptor fashion. By comparing the Raman scattering bands of Au NCs with complex **2-4** at

785 nm, the band at 1295 cm^{-1} assigned to coordinated 4,5-diazafluoren-9-one ligand ring breathing mode combined with C–O-Au linkage (Figure 4**a**).

The raman scattering band intensity was enhanced with the increase of exposure time (10 s to 120 s) for excitation at 785 nm, which indicated the enhancement of structural polarity to time (Figure S5, Supporting Information). In Au-complex 2 nanocomposites, the signal at 643, 665 cm^{-1} were assigned to asymmetric C–C bpy ring breathing, 765 cm^{-1} was assigned to bpy ring vibration with N atom-displacement, C–N stretching at 1107 cm^{-1}, COO^{-} stretching at 1361 cm^{-1}, 1486, 1556, 1601 cm^{-1} were assigned to bpy ligand stretching [17].

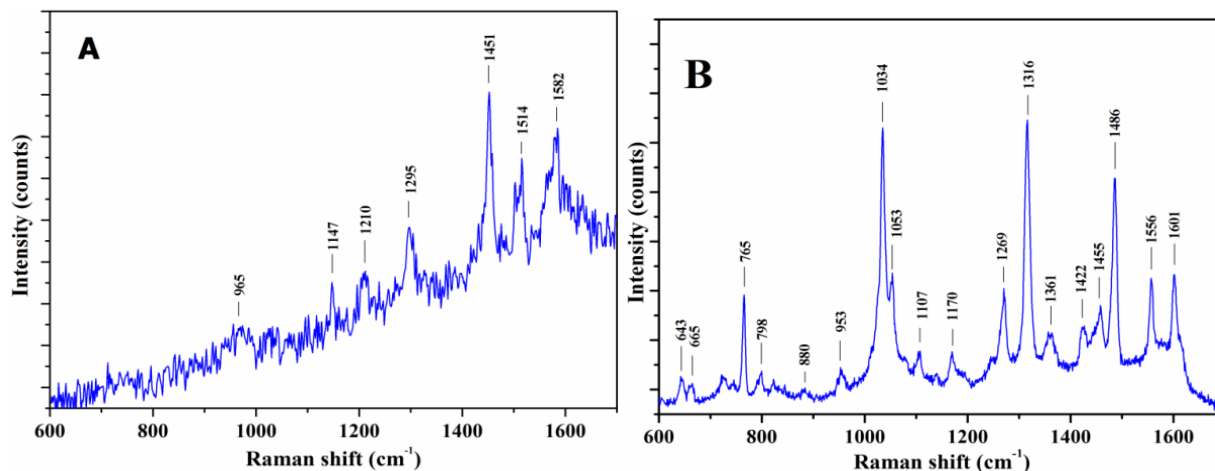**Figure 4.** a) Surface-enhanced Raman scattering signals of complex 1 @ λ_{exc}=488 nm, b) Surface-enhanced Raman scattering signals of complex 2 @ λ_{exc}=785 nm

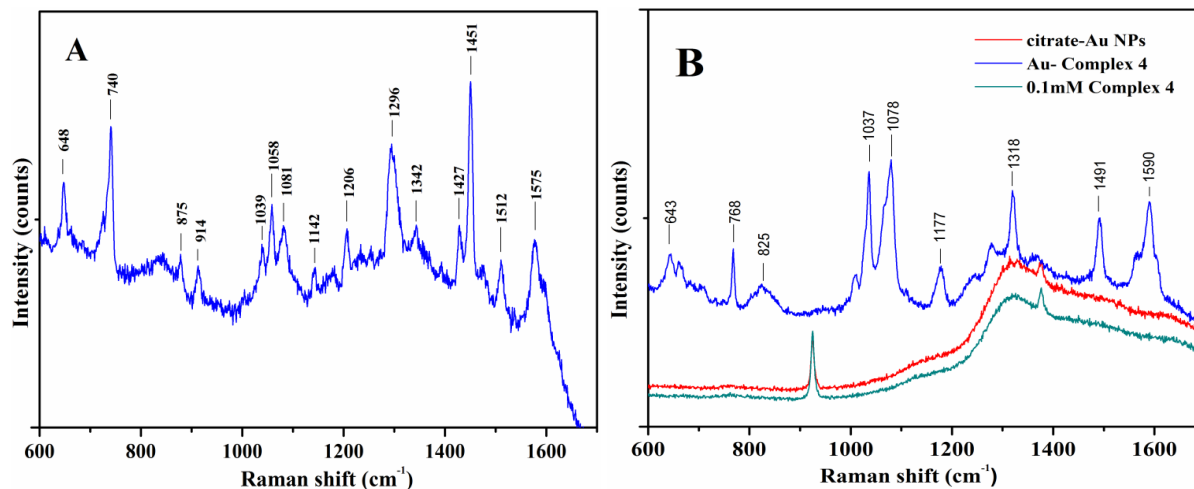**Figure 5.** a) Surface-enhanced raman scattering signals of complex 3@λ_{exc}=785 nm, b) Surface enhanced Raman scattering signals of complex 4@λ_{exc}=785 nm

The nanocomposite particles Au-complex **3** showed 648, 740, 875 were assigned to phen-ring breathing, 914 cm^{-1} was assigned to MLCT, 1142, 1206, 1296 cm^{-1} were assigned to δNH bond, 1427, 1457, 1512, 1575 cm^{-1} were assigned to phen-ring stretching mode (Figure 5**a**) [18]. In the case of functionalized Au NC formed by complex **4** molecules, Au NC was excited at 785 nm for Raman spectral responses and values represented in Figure 5**b**. By keeping the same operating condition, citrate capped Au NPs without functionalization and 0.1 mM

acetonitrile solution of complex 4 were collected to compare their Raman scattering bands. The Raman signals at 642, 662 cm^{-1} were assigned to bpy ring vibrations, 766 cm^{-1} bpy ring vibration with N-displacement, 1037, 1078, 1177, 1277, 1318 cm^{-1} were assigned to bpy and 4-ATP ring vibrations 1492, 1590 cm^{-1} were assigned to 4-aminothiophenol ring, γCC-stretching of bpy rings [19]. This scattering enhancement phenomenon was proved experimentally by recording Raman scattering with Au-Ru (1,10-phen)$_2$(IPBA).2PF$_6$

nanocomposite and Ru (1,10-phen)$_2$(4-ATP)$_2$.2PF$_6$ nanocomposite (Figure S6 and S7, Supporting Information). The covalent binding mode of complex4 enhanced the organization of Au NC particles well to provide surface-enhanced Raman scattering signals with lower concentrations. Complex **4** was bound covalently on Au surface along with Au NC particles reorganization with the functionalized surface.

Conclusions

This work demonstrated post-surface functionalization of citrate capped Au NP surface at room temperature by using various functional groups incorporated Ru(II)-polypyridyl complexes. The result of functionalized Au NCs showed selective morphology formation which was based on the nature of the functional group present in the Ru(II)-polypyridyl complex molecules introduced and its binding mode on the Au NPs surface. The surface functionalization process with citrate-capped Au NPs was unique with each Ru(II)-polypyridyl complex involved in the study proved by UV-vis spectra studies. Morphology-dependent surface-enhanced Raman scattering (SERS) signals were studied for Ru(II)-polypyridyl complex molecules. As the Au NC particles were well organized through post-functionalization, surface-enhanced Raman scattering was also noted through the hot spot mechanism. This observation indicated the importance of post-surface functionalization of Au NPs with functionalized Ru(II)-polypyridyl complexes in various binding modes to understand molecular structures even at lower than micromolar concentration. Raman scattering studies indicated the contributions of Ru(II)-polypyridyl complexes structural dependent responses at lower concentration levels and

confirmed the role of hotspot mechanism on Au NCs surface.

Acknowledgements

Disclosure Statement

No potential conflict of interest was reported by the authors.

Supporting Information

Additional supporting information related to this article can be found, in the online version, at DOI: 10.26655/AJNANOMAT.2022.2.3

References

[1]. Miomandre F., Stancheva S., Audibert J.F., Brosseau A., Pansu R.B., Lepeltier M., Mayer C.R. *J. Phys. Chem. C.*, 2013, **117**:12806 [Crossref], [Google Scholar], [Publisher]

[2]. Naeem S., Ribes A., White A.J.P., Haque M.N., Holt K.B., Wilton-Ely J.D.E.T. *Inorg. Chem.,* 2013, **52**:4700 [Crossref], [Google Scholar], [Publisher]

[3]. Elmes R.B.P., Orange K.N., Cloonan S.M., Williams D.C., Gunnlaugsson T. *J. Am. Chem. Soc.*, 2011, **133**:15862 [Crossref], [Google Scholar], [Publisher]

[4]. Abdelrahman A.I., Mohammad A.M., Okajima T., Ohsaka T. *J. Phys. Chem. B.*, 2006, **110**:2798 [Crossref], [Google Scholar], [Publisher]

[5]. Pastoriza-Santos I., Liz-Marzan L.M. *J. Mater. Chem.*, 2008, **18**:1724 [Crossref], [Google Scholar], [Publisher]

[6]. Brust M., Walker M., Bethell D., Schiffrin D.J., Whyman R. *J. Chem. Soc., Chem. Commun.*, 1994, **7**:801 [Crossref], [Google Scholar], [Publisher]

[7]. a) Liz-Marzan L.M., Giersig M., Mulvaney P. *Langmuir*, 1996, **12**:4329 [Crossref], [Google Scholar], [Publisher]; b) Mayer C.R., Dumas E., Miomandre F., Meallet-Renault R., Warmont F., Vigneron J., Pansu R., Etcheberrya A., Secheresse F. *New J. Chem.*, 2006, **30**:1628 [Crossref], [Google Scholar], [Publisher]

[8]. Moores A., Goettmann F., Sanchez C., Le Floch P. *Chem. Commun.*, 2004, 2842 [Crossref], [Google Scholar], [Publisher]

[9]. a) Halas N.J., Lal S., Chang W.S., Link S., Nordlander P. *Chem. Rev.*, 2011, **111**:3913 [Crossref], [Google Scholar], [Publisher]; b) Kelly J.J., Jespersen M.L., Vaia R.A. *J Nanopart Res.*, 2018, **20**:290 [Crossref], [Google Scholar], [Publisher]

[10]. Sullivan B.P., Salmon D.J., Meyer T.J. *Inorg. Chem.*, 1978, **17**:3334 [Crossref], [Google Scholar], [Publisher]

[11]. Yin J.F., Bhattacharya D., Thanasekaran P., Hsu C.P., Tseng T.W., Lu K.L. *Inorg. Chim. Acta.*, 2009, **362**:5064 [Crossref], [Google Scholar], [Publisher]

[12]. Henderson Jr L.J., Fronczek F.R., Cherry W.R. *J. Am. Chem. Soc.*, 1984, **106**:5876 [Crossref], [Google Scholar], [Publisher]

[13]. Grabar K.C., Freeman R.G., Hommer M.B., Natan M. *J. Anal. Chem.*, 1995, **67**:735 [Crossref], [Google Scholar], [Publisher]

[14]. Gangula A., Chelli J., Bukka S., Poonthiyil V., Podila R., Kannan R., Rao A.M. *J. Mater. Chem.*, 2012, **22**:22866 [Crossref], [Google Scholar], [Publisher]

[15]. Sun Y., Mayers B., Herricks T., Xia Y. *Nano Lett.*, 2003, **3**:955 [Crossref], [Google Scholar], [Publisher]

[16]. Leopold N., Chis V., Mircescua N.E., Maris O. T., Bujaa C.M., Leopoldb L.F., Socaciub C., Braicuc C., Irimied A., Bindan-Neagoe I. *Colloids and Surfaces A: Physicochem. Eng. Aspects.*, 2013, **436**:133 [Crossref], [Google Scholar], [Publisher]

[17]. Kokoskova M., Prochazka, M., Sloufova I., Vlckova B. *J. Phys. Chem. C.*, 2013, **117**:1044 [Crossref], [Google Scholar], [Publisher]

[18]. Abraham B., Sastri C.V., Maiya B.G., Umapathy S. *J. Raman Spectrosc.*, 2004, **35**:13 [Crossref], [Google Scholar], [Publisher]

[19]. a) Muro-Small M.L., Yarnell J.E., McCusker, C.E., Castellano F.N. *Eur. J. Inorg. Chem.,* 2012**, 2012:**4004 [Crossref], [Google Scholar], [Publisher]; b) Osawa M., Matsuda N., Yoshii K., Uchida I. *J. Phys. Chem.*, 1994, **98**:12702 [Crossref], [Google Scholar], [Publisher]